

# Metallic nanograins: spatially nonuniform pairing induced by quantum confinement

M. D. Croitoru<sup>1,3</sup>, A. A. Shanenkov<sup>2</sup>, C. C. Kaun<sup>3</sup>, and F. M. Peeters<sup>2</sup>

<sup>1</sup>*Institut für Theoretische Physik III, Universität Bayreuth, 95440 Bayreuth, Germany*

<sup>2</sup>*Departement Fysica, Universiteit Antwerpen, Groenenborgerlaan 171, B-2020 Antwerpen, Belgium and*

<sup>3</sup>*Research Center for Applied Sciences, Academia Sinica, 11529 Taipei, Taiwan*

(Dated: November 2, 2018)

It is well-known that the formation of discrete electron levels strongly influences the pairing in metallic nanograins. Here we focus on another effect of quantum confinement in superconducting grains that was not studied previously, i.e., spatially nonuniform pairing. This effect is very significant when single-electron levels form bunches and/or a kind of shell structure: in highly symmetric grains the order parameter can exhibit variations with position by an order of magnitude. Nonuniform pairing is closely related to a quantum-confinement induced modification of the pairing-interaction matrix elements and size-dependent pinning of the chemical potential to groups of degenerate or nearly degenerate levels. For illustration we consider spherical metallic nanograins. We show that the relevant matrix elements are as a rule enhanced in the presence of quantum confinement, which favors spatial variations of the order parameter, compensating the corresponding energy cost. The size-dependent pinning of the chemical potential further increases the spatial variation of the pair condensate. The role of nonuniform pairing is smaller in less symmetric confining geometries and/or in the presence of disorder. However, it always remains of importance when the energy spacing between discrete electron levels  $\delta$  is approaching the scale of the bulk gap  $\Delta_B$ , i.e.,  $\delta > 0.1-0.2 \Delta_B$ .

PACS numbers: 74.20.Fg, 74.78.Na

Keywords: metallic nanograins, nonuniform pairing, superconducting correlations, matrix elements

## I. INTRODUCTION

Quantum confinement plays a fundamental role in superconductors with nanoscale dimensions. Interplay of quantum confinement and pairing correlations results in important qualitative changes in the superconductor characteristics.<sup>1-17</sup> Because of technological reasons quasi-0D superconducting structures (i.e., ensembles of small grains) were the first where this interplay was investigated experimentally. Initial attempts by Giaever and Zeller at the end of 60s used tunneling studies on large ensembles of superconducting particles.<sup>18</sup> Since that time most of the studies on superconducting correlations in grains were performed with grain powders<sup>19,20</sup> or on films made of crystalline granules separated by amorphous inter-granular space.<sup>21,22</sup> In the pioneering work of Ralph et al.<sup>23,24</sup> the discrete electron spectrum was measured for a single grain. Their technique (single-electron tunneling spectroscopy) enabled them for the first time to probe superconducting correlations in an individual Al grain. Very recently, STM was used to detect the superconducting gap of an isolated ultra-small lead grain deposited onto a silicon substrate (see e.g. Refs. 25 and 26). These advances opened new prospects to examine superconductivity in individual metallic nanograins with unprecedented detail, e.g., to investigate the influence of the confinement on the superconducting correlations.

The main feature of a superconducting nanograin that makes them different from a bulk superconductor is the formation of discrete electron levels with average energy spacing  $\delta \approx 2\pi^2\hbar^2/(mk_F V)$ , with  $k_F$  the bulk Fermi wave number and  $V$  the system volume. It can be of the same order as the bulk gap  $\Delta_B$ , or even larger in the case

of ultra-small nanograins. Therefore, size-quantization of the electron spectrum can have a substantial impact on the basic superconducting characteristics of such quasi-0D superconducting systems.

The understanding of the fundamental properties of superconducting correlations in low-dimensional structures, in particular in isolated metallic grains, has experienced a remarkable development in the last two decades. Theoretical aspects, which have attracted the most attention are the following. The problem of the breakdown of BCS superconductivity in ultra-small metallic grains was addressed in several papers.<sup>4,27,28</sup> The effect of the shell structure in the single-electron spectrum on the superconducting correlations was pointed out for nanograins<sup>8,17</sup> and ultrasmall metallic clusters.<sup>10,11</sup> The ground state properties of the BCS pairing Hamiltonian of ultra-small grains were considered beyond the mean-field approximation using the Richardson exact solution.<sup>7-9</sup>

A spatially uniform pairing was assumed in these and other works and, as a consequence, the matrix elements of the pairing interaction were taken independent of the relevant single-electron quantum numbers, i.e., they were set to  $-g/V$ , with  $g > 0$  the coupling constant and  $V$  the volume.<sup>29</sup> This is, say, a bulk-like approximation recovered when the single-electron wave functions are taken as plane waves. However, the translational invariance is broken in nanograins, which leads to a position-dependent order parameter. As a result, the pairing gap becomes strongly dependent on the relevant quantum numbers, which is directly related to a confinement-induced modification (as compared to  $-g/V$ ) of the matrix elements controlling the scattering of the time reversed states. An-

other important issue is that single-electron levels can form bunches and even a kind of shell structure in symmetric confining geometries. In this case the chemical potential  $\mu$  can be pinned to a group of nearly degenerate or degenerate levels. This is of importance because the density of states in the vicinity of  $\mu$  strongly influences the superconducting correlations. In other words, such a pinning plays the role of a filter that selects the contribution of a particular single-electron shell (or of a group of close levels) to the superconducting order parameter. Such a contribution is, as a rule, spatially nonuniform.

The aim of the present paper is to investigate effects related to a spatially nonuniform pairing in metallic nanograins, which was not studied in previous publications. For illustrative purposes we consider metallic spherical nanograins, where the spatial dependence of the superconducting condensate is pronounced (the order parameter can vary with position by an order of magnitude). In less symmetric confining geometries and/or in the presence of disorder spatial variations of the order parameter are reduced. However, our study implies that nonuniform pairing remains of importance when the interlevel spacing  $\delta$  is approaching the scale of the order of the bulk gap  $\Delta_B$ . Any remaining grouping of single-electron levels, that is always present in real samples, even strengthens the effect of interest. We work in the mean-field approximation and, thus, stay in the regime  $\delta \lesssim \Delta_B$ . Below we consider Sn and Al with  $\Delta_B = 0.616$  and  $0.25$  meV, respectively (for the parameters used below). Using the above values of  $\Delta_B$ , we find that the mean-field approach is valid for  $D > 6$ -8 nm, with  $D$  the sphere diameter.

Our paper is organized as follows. In Sec. II, we outline the formalism how to obtain a self-consistent solution to the problem. In Sec. III, we present our numerical results. In particular, in Sec. III A we investigate the effects of quantum confinement on pairing correlations through the modifications of the matrix elements of the pairing interaction and the size-dependent pinning of  $\mu$  to single-electron shells. Sec. III B is focused on a spatial distribution of the pair condensate and its relation to modifications of the matrix elements and the size-dependent pinning of  $\mu$ . In Sec. III C we discuss the interplay of Andreev reflection with quantum confinement, resulting in the formation of Andreev-type states and significant dependence of the pairing gaps on the relevant quantum numbers. A short summary and discussion are given in Sec. IV.

## II. FORMALISM

The reduction of the system to the nanometer scale leads to the formation of a discrete electron spectrum. Moreover, in the presence of quantum confinement, the translational invariance of the system is broken, and the superconducting order parameter is position dependent, i.e.,  $\Delta = \Delta(\mathbf{r})$ . For the mean-field treatment of such

a situation, it is appropriate to use the Bogoliubov-de Gennes (BdG) equations,<sup>31,32</sup> which can be written as

$$E_i|u_i\rangle = \hat{H}_e|u_i\rangle + \hat{\Delta}|v_i\rangle, \quad (1a)$$

$$E_i|v_i\rangle = \hat{\Delta}^*|u_i\rangle - \hat{H}_e^*|v_i\rangle, \quad (1b)$$

where  $E_i$  stands for the Bogoliubov-quasiparticle (bogolon) energy,  $\hat{\Delta} = \Delta(\hat{\mathbf{r}})$  (with  $\hat{\mathbf{r}}$  the position operator) and the single-electron Hamiltonian is referred to the chemical potential  $\mu$ , i.e.,

$$\hat{H}_e(\mathbf{r}) = \frac{\hat{\mathbf{p}}^2}{2m_e} + V(\hat{\mathbf{r}}) - \mu. \quad (2)$$

We remark that any magnetic effects are beyond the scope of the present paper. For simplicity, the confining interaction  $V(\mathbf{r})$  is taken as zero inside the specimen and infinite outside:  $V(\mathbf{r}) = V_B \vartheta(R - \rho)$  with the barrier potential  $V_B \rightarrow \infty$  ( $R = D/2$  and  $\rho$  is the radial coordinate for the spherical confining geometry).

As a mean-field approach, the BdG equations should be solved in a self-consistent manner

$$\Delta(\mathbf{r}) = g \sum_i \langle \mathbf{r}|u_i\rangle \langle v_i|\mathbf{r}\rangle \tanh\left(\frac{\beta E_i}{2}\right), \quad (3)$$

where  $g > 0$  is the coupling constant for the effective electron-electron interaction approximated by the delta-function potential, i.e.,  $\langle \mathbf{r}, \mathbf{r}'|\Phi|\mathbf{r}, \mathbf{r}'\rangle = -g\delta(\mathbf{r} - \mathbf{r}')$ . The sum in Eq. (3) runs over the states with the single-electron energy

$$\xi_i = [\langle u_i|\hat{H}_e|u_i\rangle + \langle v_i|\hat{H}_e|v_i\rangle] \in [-\hbar\omega_D, \hbar\omega_D], \quad (4)$$

with  $\omega_D$  the Debye frequency. As is known, the solution of the BdG equations has two branches:  $(i, +)$  and  $(i, -)$  (see Ref. 33) for which we have  $E_{i,+} > 0$  and  $E_{i,-} < 0$ . The sum in Eq. (3) should be taken over the physical states [the  $(i, +)$  branch], i.e.,  $E_i = E_{i,+}$ .

For a given mean electron density  $n_e$  the chemical potential  $\mu$  is determined from

$$n_e = \frac{2}{V} \sum_i [f_i \langle u_i|u_i\rangle + (1 - f_i) \langle v_i|v_i\rangle], \quad (5)$$

with  $V = \frac{4}{3}\pi R^3$  the volume of the spherical grain. For conventional superconductors the energy gap is typically much smaller than the chemical potential. As a result,  $\mu$  stays nearly the same when passing from the normal state to the superconducting one.<sup>32</sup> Therefore, one can solve Eq. (5) in the absence of superconducting order ( $\Delta(\mathbf{r}) = 0$ ).

In a spherical nanograin, because of symmetry reasons, the order parameter depends only on the radial coordinate, i.e.,  $\Delta = \Delta(\rho)$ . Therefore the pseudospinor in the particle-hole space can be characterized by the quantum numbers of the angular momentum, i.e.,  $(l, m)$ . The angular part of the pseudospinor  $\Psi_i$  is given by the spherical harmonics  $Y_{lm}(\theta, \varphi)$  in polar coordinates  $(\rho, \theta, \varphi)$ , i.e.,

$$\langle \mathbf{r}|\Psi_i\rangle = Y_{lm}(\theta, \varphi) \begin{pmatrix} u_{jl}(\rho) \\ v_{jl}(\rho) \end{pmatrix}, \quad (6)$$

where  $i = \{j, l, m\}$ , with  $j$  the radial quantum number associated with the quantum-confinement boundary conditions

$$u_{jl}(\rho)|_{\rho=R} = v_{jl}(\rho)|_{\rho=R} = 0. \quad (7)$$

To solve the BdG equations (1a) and (1b) numerically,  $u_{jl}(\rho)$  and  $v_{jl}(\rho)$  are expanded in the eigenfunctions of the single-electron Hamiltonian  $\widehat{H}_e$  [see Eq. (2)]. In addition, iterations should be invoked, to account for the self-consistency relation given by Eq. (3). This program is significantly simplified by keeping only the pairing of the time-reversed states,<sup>34</sup> which is a standard approximation for the problem of superconducting correlations in nanograins. In the framework of the BdG equations this can be done through the so-called Anderson approximate solution for which the particle- and hole-like wave functions are assumed to be proportional to the single-electron wave function. It means that

$$u_{jl}(\rho) = \mathcal{U}_{jl} \chi_{jl}(\rho), \quad u_{jl}(\rho) = \mathcal{V}_{jl} \chi_{jl}(\rho), \quad (8)$$

with the radial part of the single-electron wave function given by

$$\chi_{jl}(\rho) = \frac{\sqrt{2}}{R^{3/2} j_{l+1}(\alpha_{jl} \frac{\rho}{R})} j_l(\alpha_{jl} \frac{\rho}{R}), \quad (9)$$

with  $j_l(x)$  the  $l$ -order spherical Bessel function of the first kind and  $\alpha_{jl}$  its  $j$ -node. The coefficients  $\mathcal{U}_{jl}$  and  $\mathcal{V}_{jl}$  (taken as real) obey the standard constraint (see, e.g., Refs. 35)

$$\mathcal{U}_{jl}^2 + \mathcal{V}_{jl}^2 = 1. \quad (10)$$

Then, inserting Eq. (8) into Eqs. (1a) and (1b) we find the following set of coupled equations (here  $E_{jlm} = E_{jl}$  and  $\xi_{jlm} = \xi_{jl}$ ):

$$[E_{jl} - \xi_{jl}] \mathcal{U}_{jl} = \Delta_{jl} \mathcal{V}_{jl}, \quad (11a)$$

$$[E_{jl} + \xi_{jl}] \mathcal{V}_{jl} = \Delta_{jl} \mathcal{U}_{jl}, \quad (11b)$$

with

$$\Delta_{jl} = \int_0^R d\rho \rho^2 \chi_{jl}^2(\rho) \Delta(\rho) \quad (12)$$

and

$$\xi_{jl} = \frac{\hbar^2}{2m_e} \frac{\alpha_{jl}^2}{R^2} - \mu. \quad (13)$$

A nontrivial physical solution of Eqs. (11a) and (11b) exists only when

$$E_{jl} = \sqrt{\xi_{jl}^2 + \Delta_{jl}^2}. \quad (14)$$

The Anderson prescription about the pairing of the time-reversed states allows one to rephrase the self-consistency relation [see Eq. (3)] as follows:

$$\Delta_{j'l'} = - \sum_{jl} (2l+1) \frac{M_{j'l',jl} \Delta_{jl}}{2\sqrt{\xi_{jl}^2 + \Delta_{jl}^2}} \tanh\left(\frac{\beta E_{jl}}{2}\right), \quad (15)$$

where

$$M_{j'l',jl} = -\frac{g}{4\pi} \int_0^R d\rho \rho^2 \chi_{j'l'}^2(\rho) \chi_{jl}^2(\rho).$$

To derive Eq. (15), one should keep in mind the property of the spherical harmonics  $\sum_{m=-l}^l |Y_{lm}(\theta, \varphi)|^2 = \frac{2l+1}{4\pi}$ . We remark that  $M_{j'l',jl}$  is nothing else but the pairing-interaction matrix element  $\langle i', \bar{i}' | \Phi | i, \bar{i} \rangle$  (with  $\bar{i} = \{j, l, -m\}$ ) averaged over the states with  $m = -l, \dots, l$  and  $m' = -l', \dots, l'$ , i.e.,

$$M_{j'l',jl} = \frac{1}{(2l'+1)(2l+1)} \sum_{m'=-l'}^{l'} \sum_{m=-l}^l \langle i', \bar{i}' | \Phi | i, \bar{i} \rangle.$$

As seen from Eq. (12), a spatially uniform order parameter means that the pairing gaps  $\Delta_{jl}$  do not depend on the quantum numbers  $j$  and  $l$ . This is compatible with Eq. (15) only when  $M_{j'l',jl}$  does not depend on  $j'$  and  $l'$ . According to the definition given by Eq. (16), we have  $M_{j'l',jl} = M_{jl,j'l'}$  and, so, if  $M_{j'l',jl}$  does not depend on  $j', l'$ , it does not depend on  $j, l$  either. So, we arrive at the standard simplified approach of investigating the pairing correlations in metallic grains (see the discussion in the Introduction). Below we show that the spatial dependence of the order parameter can not be ignored in superconducting nanograins, which implies significant variations of the matrix elements and pairing gaps with the relevant quantum numbers. After a numerical solution of Eq. (15), the position-dependent order parameter can be calculated from

$$\Delta(\rho) = \sum_{jl} \Delta^{(jl)}(\rho), \quad (16)$$

with the shell-dependent contribution  $\Delta^{(jl)}(\rho)$  given by

$$\Delta^{(jl)}(\rho) = \frac{g}{8\pi} (2l+1) \frac{\chi_{jl}^2(\rho) \Delta_{jl}}{\sqrt{\xi_{jl}^2 + \Delta_{jl}^2}} \tanh\left(\frac{\beta E_{jl}}{2}\right). \quad (17)$$

### III. DISCUSSION OF RESULTS

#### A. Enhanced intrashell matrix elements and quantum-size pinning of the chemical potential

Numerical calculations were performed with the set of parameters typical for tin<sup>32,36</sup>:  $\hbar\omega_D/k_B = 195$  K,  $gN(0) = 0.25$ , with  $N(0)$  the bulk density of states at the Fermi level (we use the bulk electron density  $n_e = 148 \text{ nm}^{-3}$ , see, e.g., Ref. 37).

Figure 1(a) shows the critical temperature (in units of the bulk critical temperature  $T_{c,B}$ ) versus the nanograin diameter  $D$  as calculated from Eq. (15) when the matrix elements of the electron-electron interaction and the size-dependent variation of the chemical potential have been

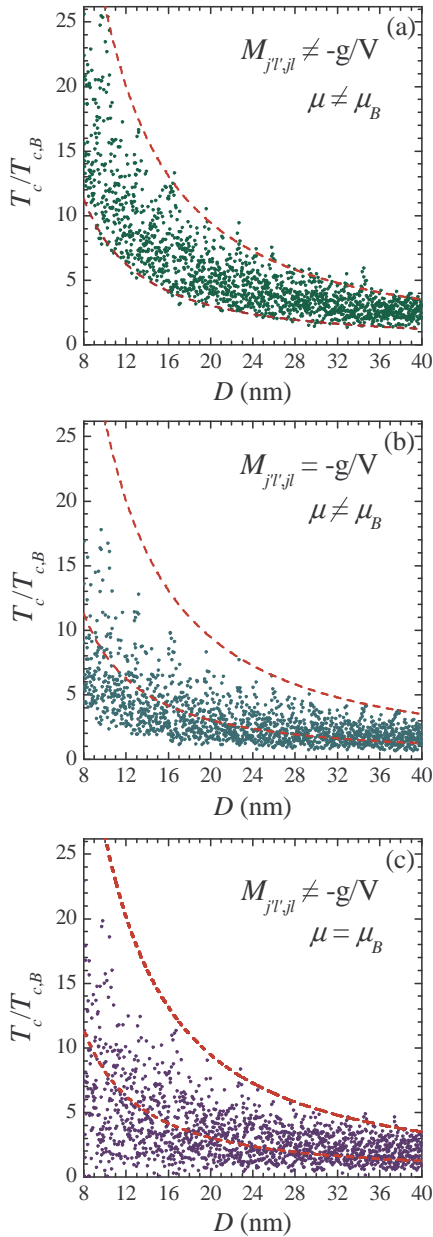


FIG. 1. Critical temperature versus the grain diameter as calculated for: (a)  $M_{j'l',jl} \neq -g/V$  and  $\mu \neq \mu_B$ ; (b)  $M_{j'l',jl} = -g/V$  and  $\mu \neq \mu_B$ ; and (c)  $M_{j'l',jl} \neq -g/V$  and  $\mu = \mu_B$ . The dashed curves in (a) show approximate lower and upper boundaries for the quantum-size oscillations of  $T_c$ , both curves represent the same dependence  $T_c/T_{c,B} = 1 + a(D/D_0)^{3/2}$ , with  $D_0 = 50$  nm and  $a = 1$  (the lower boundary) and  $a = 3.5$  (the upper one). The same curves are also given in (b) and (c), for comparison.

fully taken into account. Results in Fig. 1 are presented for a step  $\Delta R = 0.01$  nm. For each radius the critical temperature was defined as the temperature above which the spatially-averaged order parameter  $\langle \Delta(\rho) \rangle$  becomes smaller than 0.01 of its value at  $T = 0$ . Our numerical results exhibit two features typical of the size-dependent

pairing characteristics in high-quality superconducting nanograins and nuclei. First, we observe an overall increase of  $T_c$  with decreasing  $D$  (it is very pronounced due to the highly-symmetric confining geometry). Second,  $T_c$  oscillates wildly with  $D$ . This oscillatory behavior can be understood in the following way. The pair correlations are nonzero only for the states within a finite range (the Debye window) around the chemical potential  $\mu$ . Moreover, the main contribution to the sum in Eq. (15) comes from the states in the very vicinity of the Fermi level, because in this case the expression  $\Delta_{jl}/\sqrt{\xi_{jl}^2 + \Delta_{jl}^2} \simeq 1$  ( $\xi_{jl} \simeq 0$ ). When varying the nanograin size, the number of states in the Debye window changes. The smaller the diameter, the smaller the number of relevant states contributing to the pairing characteristics and, as a result, the more significant is such a change. This change is not monotonous but rather oscillating due to a permanent competition between incoming and outgoing states. As a consequence, all basic pairing characteristics, e.g.,  $T_c$  and pairing gaps  $\Delta_{jl}$ , exhibit quantum-size oscillations. It is not only typical of nanograins with superconducting correlations (see, e.g., the recent paper<sup>26</sup>) but it is also present in superconducting nanowires<sup>12–16</sup> and nanofilms.<sup>38,39</sup> Such oscillations are pronounced for small diameters/thicknesses but decay with increasing the characteristic size so that  $T_c$  approaches the bulk critical temperature  $T_{c,B}$  (for our parameter  $T_{c,B} = 4.01$  K). It is interesting to note that the overall increase of  $T_c$  with decreasing  $D$  in Fig. 1(a) is similar to a size-dependent enhancement of the pairing gap in nuclei, where it is proportional to  $1/\sqrt{A}$  (see, e.g., Ref. 40), with  $A$  the number of nucleons. In particular, the two dashed curves in Fig. 1(a) show approximate upper and lower boundaries for  $T_c$ , highlighting the magnitude of the quantum-size oscillations: both curves represent the same dependence, i.e.,  $T_c/T_{c,B} = 1 + a(D/D_0)^{3/2}$ , with  $D_0 = 50$  nm and  $a = 1$  and 3.5 for the lower and upper boundaries, respectively [ $(D_0/D)^{3/2} \propto N_e^{-1/2}$ , with  $N_e = n_e V$  the number of electrons]. We remark that real samples exhibit inevitable shape and size fluctuations that affect the high-degeneracy of single-electron levels. Hence, measurements on an ensemble of nanograins will significantly smooth the quantum-size oscillations in the critical temperature and reduce its overall enhancement with decreasing nanograin size (see, also, Sec. IV). For instance, in experimentally fabricated tin nanograins of a semi-spherical shape the observed enhancement of the excitation gap over its bulk value is about<sup>26</sup> 60% for the particle heights  $\approx 10$ -20 nm. This is significantly smaller than the enhancement of  $T_c$  shown in Fig. 1(a). However, detailed investigations of the enhancement of  $T_c$  in superconducting nanograins is beyond the scope of our present paper. Here we are interested in a spatially nonuniform distribution of the pair condensate which is of importance even in the presence of shape and size fluctuations and disorder (see the discussion in Sec. IV).

In order to outline the role of the matrix elements

$M_{j'l',jl}$  [see Eq. (16)] of the electron-electron interaction we also show what happens when the true matrix elements are simply replaced by those of the bulk-like form:  $M_{j'l',jl} = -g/V$ , which is what is usually done when investigating the superconducting correlations in nanograins. The results are displayed in Fig. 1(b) and, as seen, the difference with respect to Fig. 1(a) is significant. To simplify the comparison, we show also in Fig. 1(b) two solid curves that represent the radius-dependent upper and lower values of  $T_c$  from Fig. 1(a).

TABLE I. Matrix elements  $M_{j'l',jl} = M_{jl,j'l'}$  in units of  $-g/V$  calculated at  $D = 7.1$  nm for quantum numbers such that  $\xi_{j'l'}, \xi_{jl} < \hbar\omega_D$ :

$M_{j'l',jl}$	$j'$	$l'$	$j$	$l$
10.62	31	11	31	11
1.9	31	11	23	29
1.33	31	11	19	39
0.64	31	11	8	71
0.41	31	11	1	101
4.71	23	29	23	29
1.7	23	29	19	39
0.7	23	29	8	71
0.43	23	29	1	101
3.72	19	39	19	39
0.77	19	39	8	71
0.46	19	39	1	101
2.69	8	71	8	71
0.69	8	71	1	101
3.61	1	101	1	101

To clarify the physical reason why using the true matrix elements leads to significant deviations from the results found for  $M_{j'l',jl} = -g/V$ , we show in Table I the numerical values of  $M_{j'l',jl}$  (calculated in units of  $-g/V$ ) for  $D = 14.2$  nm (only the states within the Debye window are given). As seen, the diagonal (intrashell) matrix elements  $M_{jl,jl}$  are strongly enhanced as compared to  $-g/V$ . However, the matrix elements controlling the scattering of the time reversed states between different shells (intershell) are often decreased in absolute value with respect to  $-g/V$ . So, the question arises why the superconducting correlations are enhanced for the true matrix elements? The point is that the intershell interactions are of less importance due to a size-dependent pinning of the chemical potential to the groups of degenerate or nearly degenerate levels (shells can be often close to each other in energy), see the next paragraph. When  $\mu$  is pinned to a particular shell, then the single-electron energy measured from  $\mu$  is zero for the states from this shell. These states make a major contribution to superconducting correlations unless diameters are not large enough  $D < 20$ -30 nm, in other words, the number of contributing shells is less than 10-15. In this case the superconducting correlations are nearly determined by the pairing gap  $\Delta_{jl}$  associated with the shell pinned

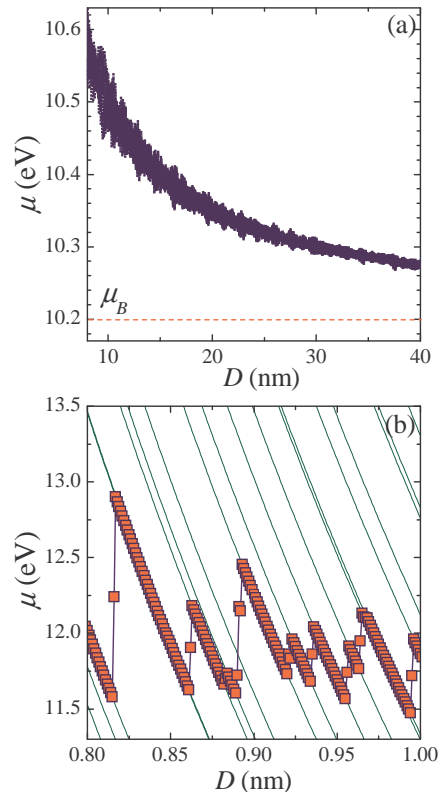


FIG. 2. (a) Size variations of the chemical potential, accompanied by an overall shift of  $\mu$  to upper values with decreasing  $D$ . (b) Details of the quantum-size pinning of  $\mu$  (filled squares) to the single-electron levels (solid curves), small diameters are shown for simplicity.

to  $\mu$ . From Eq. (15) it is seen that  $\Delta_{jl}$  for the states with  $\xi_{jl} = 0$  is mainly governed by the intrashell matrix element  $M_{jl,jl}$ . For instance, when ignoring the contribution of all other states one simply obtains (at  $T = 0$ )

$$\Delta_{jl} \approx -\left(l + \frac{1}{2}\right) M_{jl,jl}.$$

When the diameter increases beyond 20-30 nm, then the intershell matrix elements approach  $-g/V$  while the intrashell matrix elements are still significantly different from the bulk-like behavior. However, the role of the states with  $\xi_{jl} = 0$  is becoming less and less important for larger diameters due to the presence of larger and larger number of shells making a contribution to the pairing correlations. As a consequence, the difference between the data in Figs. 1(a) and (b) decreases when approaching  $D = 35$ -40 nm, together with the amplitude of the quantum-size oscillations of  $T_c$ .

In the fully self-consistent scheme the chemical potential is determined in such a way that the mean electron density  $n_e$  is constant [see Eq. (5)]. However, size-dependent variations of  $\mu$  are of importance not only because they simply prevent the mean electron density from deviations. In fact, such deviations are almost insignificant: our calculations for  $\mu = \mu_B$  show that  $n_e$  decreases

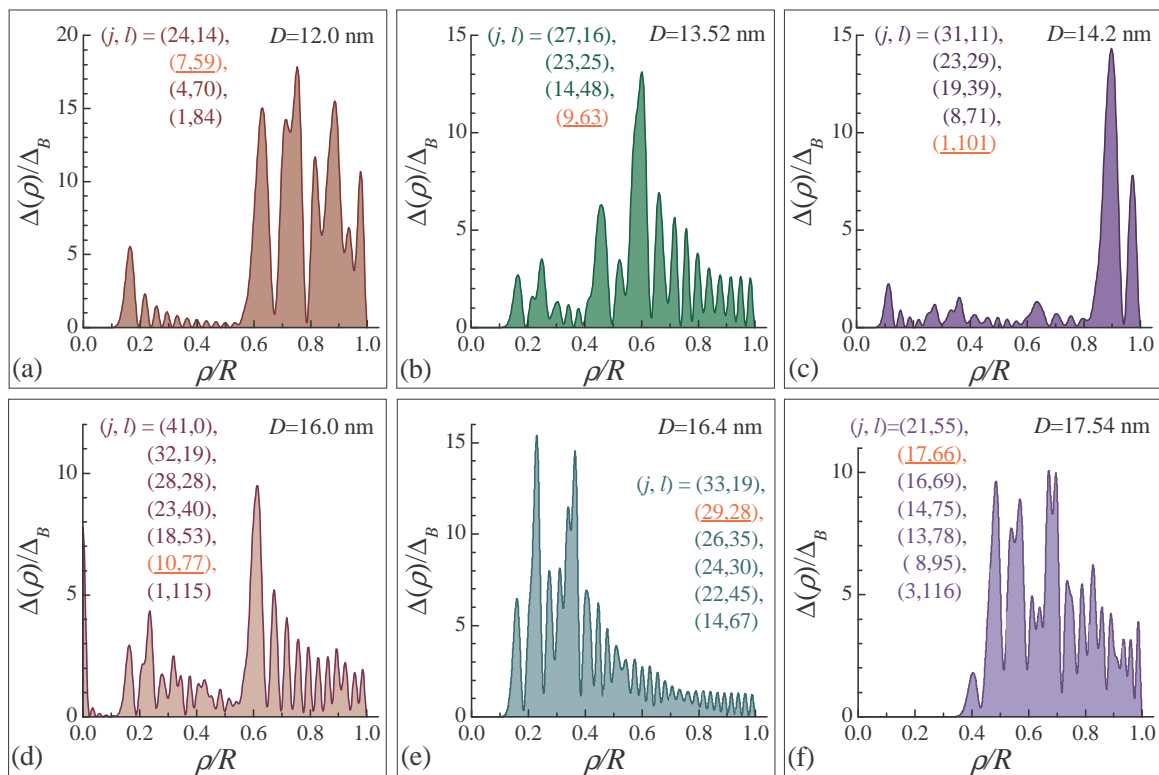


FIG. 3. Spatial distribution of the pair condensate in spherical nanograins:  $\Delta(\rho)$  (calculated at  $T = 0$ ) versus  $\rho$  for diameters  $D = 12$  nm (a), 13.52 nm (b), 14.2 nm (c), 16 nm (d), 16.4 nm (e) and 17.54 nm (f).

by a few percent when  $D$  reduces to 10-20 nm. A more interesting thing is that the size-dependent variations of  $\mu$  have a pronounced effect on the superconducting correlations. In particular, this can be seen from Fig. 2(c), where  $T_c$  is calculated for the true matrix elements and  $\mu = \mu_B$ . What is the reason for this suppression of  $T_c$ ? In the presence of the formation of strongly degenerate electron levels or bunches of electron levels with almost negligible spacing between them, the chemical potential lies mostly at the highest partly-filled degenerate level (see, e.g., Refs. 10 and 11). Pairing correlations are significant only within the Debye window around the chemical potential  $\mu$  and are strongest<sup>27</sup> exactly at  $\mu$ . Hence, when  $\mu$  is pinned to a shell level, this favors the pairing correlations at this level and, in turn, through the self-consistency relation, favors the pairing correlations at neighboring shells. In other words, if the level to which the chemical potential is pinned is highly degenerate than the phase space for the strongest pair scattering is enlarged and, consequently, the system gains in interaction energy and, as a result, superconducting correlations are strongly enhanced. It is different when  $\mu$  is not pinned to a shell, which is mostly the case for a constant chemical potential, e.g., for  $\mu = \mu_B$ . Here the relevant shells entering the Debye window are as a rule specified by  $\xi_{jl} \neq 0$  and, so, their contributions are diminished.

The above discussion is further illustrated by our nu-

merical results for  $\mu$  in Fig. 2. As seen from panel (a), when keeping the electron density of the system constant,  $\mu$  slightly shifts systematically up with decreasing  $D$  and exhibits size-dependent oscillations, as seen from Fig. 2(a). These oscillations are a signature of the size-dependent pinning of  $\mu$  to groups of degenerate or nearly degenerate single-electron levels. This is clearly seen from Fig. 2(b), where variations of  $\mu$  (filled squares) are plotted versus  $D$  together with the single-electron energies measure from the band bottom, i.e.,  $\frac{\hbar^2}{2m_e} \frac{\alpha_{jl}^2}{R^2}$  (solid curves). For the sake of simple illustration, panel (b) shows the data for extremely small diameters, where the energy spacing between the shell levels is pronounced and, as a result, the size-dependent oscillations of  $\mu$  are not so wild as it happens for higher diameters. As follows from Fig. 2(b)  $\mu$  is pinned to a shell level in most cases, which, as mentioned above, represents incomplete shells. Sometimes  $\mu$  can be found between two neighboring shell levels, which corresponds to the case of a fully occupied lower shell.

## B. Spatially nonuniform pair condensate

In the previous paragraph we considered the effect of quantum confinement on pairing correlations through the matrix elements and quantum-size pinning of  $\mu$ . As dis-

cussed at the end of Sec. II, a framework which incorporates both issues appears to be only consistent when the position-dependent superconducting order parameter is taken into consideration. Thus, our results discussed in the previous section suggest that the spatial variations of  $\Delta(\rho)$  will be pronounced even in nanograins with diameters up to  $D = 20\text{-}30\text{ nm}$ . However, it is usually argued that spatial variations of  $\Delta(\rho)$  cost significant extra energy and, so, they are strongly suppressed when  $D \ll \xi$ , with  $\xi$  the bulk coherence length (see, for instance, Ref. 28). In addition,  $D$  should be larger than  $\lambda_F$ : in practice,  $k_F D \sim 10$  is assumed to be sufficient to ignore any spatial dependence of the order parameter.<sup>10,11</sup> For typical metallic parameters  $k_F D \sim 200\text{-}400$  for  $D = 10\text{-}20\text{ nm}$  and this is the reason why the spatial dependence of the order parameter was ignored in most papers on superconducting correlations in nanograins. To go in a more detail on this point, we below discuss our numerical results on  $\Delta(\rho)$ .

In Fig. 3 the radial dependence of the superconducting order parameter is shown as calculated from Eq. (16) for  $D = 12\text{ nm}$  (a),  $13.52\text{ nm}$  (b),  $14.2\text{ nm}$  (c),  $16\text{ nm}$  (d),  $16.4\text{ nm}$  (e) and  $17.54\text{ nm}$  (f). The shells making a contribution to the superconducting correlations are also displayed in each panel, and the quantum numbers of the shell level pinned to  $\mu$  are underlined. As seen, we in general have a nonuniform distribution of the pair condensate for diameters  $D = 10\text{-}20\text{ nm}$ , which is in agreement with our expectations. For example, let us consider the results plotted in panel (c). Here  $\mu$  is pinned to the shell level  $(l, j) = (101, 1)$  and, so, single-electron states with  $j = 1$  and  $l = 101$  make a major contribution to  $\Delta(\rho)$ , which results in a significant enhancement of the order parameter next to the edge, i.e., for  $\rho/R = 0.9\text{-}1.0$ . The profile of this enhancement is determined by the radial wave function  $\chi_{1,101}^2(\rho)$  with two pronounced local maxima ( $\Delta/\Delta_B = 14.3$  and  $7.2$  at  $\rho/R = 0.9$  and  $0.97$ , respectively) and one node (recall that  $j$  is the number of the nodes of the radial wave function). All the other shells displayed in Fig. 3(c) are specified by  $\xi_{jl} \neq 0$  and, as a result, their contributions is much less significant. The local maximum  $\Delta(\rho)/\Delta_B = 2.3$  at  $\rho/R = 0.1$  is due to states  $(j, l) = (31, 11)$ . The shells with  $(j, l) = (23, 29)$  and  $(19, 29)$  are responsible for local enhancements of the order parameter up to  $1.5\text{-}2.0\Delta_B$  at  $\rho/R = 0.27$  and  $0.36$ , respectively. At last, the shell  $(8, 71)$  produces the local maximum at  $\rho/R = 0.64$ . In general, the larger the angular momentum, the larger the values of  $\rho/R$  at which the corresponding single-electron states have an effect on the profile of  $\Delta(\rho)$ .

It is worth noting that typically, the order parameter is strongly suppressed in the center ( $\rho = 0$ ) except of rare cases when states with zero angular momentum contribute to the pairing correlations. One such example is given in Fig. 3(d), where a narrow pick can be seen at  $\rho = 0$  due to the contribution of the shell with  $(j, l) = (41, 0)$ .

From Fig. 3 it follows that the radial distribution of

the pair condensate remains strongly nonuniform even for  $D \approx 20\text{ nm}$ . We would like to note that when selecting concrete values of  $D$  for Fig. 3, we did not even take diameters for which  $T_c$  is close to the upper dashed curve in Fig. 1(a). In the case of a strong enhancement of  $T_c$  the radial distribution of the pair condensate is as a rule strongly nonuniform. The points selected for Fig. 3 are mainly in a vicinity of the lower dashed curve in panel (a) of Fig. 1: for  $D = 13.52, 14.2, 16$  and  $16.4\text{ nm}$  we have  $T_c/T_{c,B} = 6.41, 6.48, 4.082$  and  $3.78$ , respectively. However, even in this case the order parameter can vary with position by an order of magnitude. Spatial variations of  $\Delta(\rho)$  are significantly relaxed only when  $D$  approaches  $30\text{-}40\text{ nm}$ , as seen from Fig. 4.

For our parameters  $k_F = 16.4\text{ nm}$  and, so, we obtain  $k_F D \approx 300$  for  $D \approx 20\text{ nm}$ . Hence, the criterion  $k_F D \gg 1$  is not very useful in order to estimate the effect of spatial variations of the pair condensate. Based on our numerical study, we would like to suggest another criterion related to a more sensitive energy scale, which in the superconducting state is governed by the bulk pairing gap  $\Delta_B$ . The spatial distribution of the order parameter is always strongly inhomogeneous when  $\delta \sim \Delta_B$  (here it is even better to replace  $\Delta_B$  by the size-dependent pairing gap). The spatial variations decay with a decrease in the ratio of the mean interlevel spacing to the bulk order parameter, i.e.,  $\delta/\Delta_B$ , and our numerical results suggest that such variations are significantly reduced only when  $\delta/\Delta_B < 0.05\text{-}0.1$  (recall that effects of a magnetic field are beyond the scope of our paper). For Sn spherical superconducting grains this regime is achieved when  $D > 40\text{-}50\text{ nm}$  (note that  $\delta \approx 2\pi^2\hbar^2/(mk_F V)$  underestimates the intershell spacing for spherical confining potential). Despite that our results are for a highly symmetric confining geometry, we can expect that the order parameter will be always spatially nonuniform for  $\delta/\Delta_B > 0.1$ , even when shape imperfections and disorder dissolve a shell structure. The reason is that the number of contributing states (i.e., the states in the energy interval  $\approx [\mu - \Delta_B, \mu + \Delta_B]$ ) is not very large for  $\delta/\Delta_B > 0.1$ . In this case the states pinned to  $\mu$  always make a major contribution to the order parameter and, so, the profile of the squared absolute value of the corresponding wave function will mainly determine the spatial distribution of the condensate. Thus, the domain  $\delta/\Delta_B = 0.1\text{-}1.0$  is in general characterized by strong effects due to the spatially nonuniform pairing.

We remark that our conclusions do not contradict the usual argument that spatial variations of the order parameter cost extra energy. Let us compare a bulk superconductor with a superconducting nanograin. In bulk the relevant matrix elements controlling the scattering of the time-reversed states are  $-g/V$  and the order parameter is spatially uniform (in the absence of a magnetic field). As opposed to bulk, the pair condensate significantly varies with position in nanograins, which results, of course, in an increase of the kinetic energy. However, the intrashell matrix elements are now enhanced in absolute value as

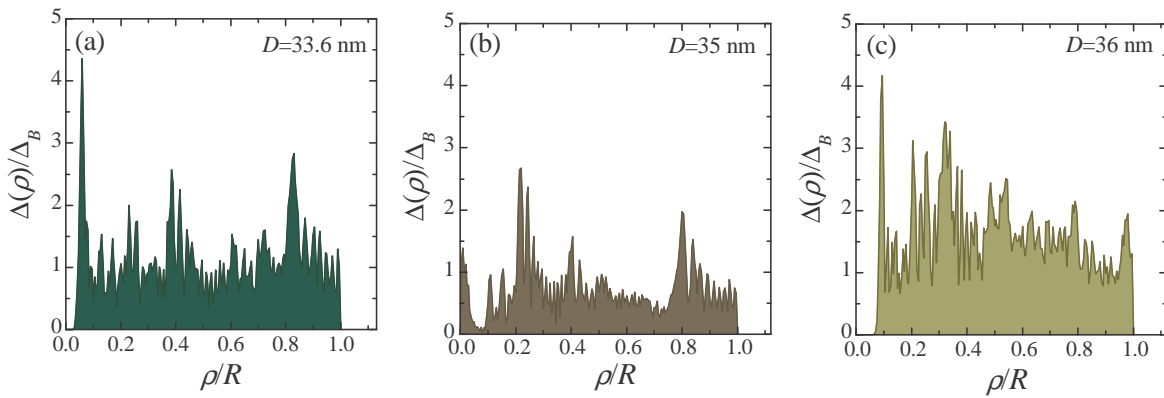


FIG. 4. The order parameter  $\Delta(\rho)$  for sufficiently large diameters  $D = 33.6$  nm (a),  $D = 35$  nm (b) and  $D = 36$  nm (c).

compared to  $-g/V$  due to quantum confinement. This compensates energy costs of spatial variations of the order parameter.

The discussion in the previous paragraph is also related to arguments that invoke the conventional Ginzburg-Landau theory. According to this arguments the order parameter is uniform in samples with size smaller than the bulk coherence length. When applying this to nanograins, one can conclude that the pair condensate should not vary with its position. However, this is not true. It is well-known that one should be careful when applying the conventional Ginzburg-Landau theory to superconductors with characteristic size smaller than the zero-temperature (BCS) coherence length  $\xi_0$ . Strictly speaking, Gor'kov's derivation of the conventional Ginzburg-Landau formalism from the BCS approach is not applicable on a scale smaller than  $\xi_0$  (see, e.g., Ref. 36). For Sn we have  $\xi_0 \approx 230$  nm (see, e.g., Ref. 32). Thus, in the case of interest  $D \ll \xi_0$ , and one can hardly invoke the conventional Ginzburg-Landau formalism to check whether or not  $\Delta(\rho)$  varies with  $\rho$ .

### C. Confinement-induced Andreev-type states

Here we would like to discuss one more issue related to a spatially nonuniform pairing in nanograins. This is the formation of Andreev-type states induced by quantum confinement<sup>14,45</sup> (see also a similar paper<sup>41</sup> discussing Andreev-type states in an ultracold trapped superfluid Fermi gas). Since the 60s (see Refs. 42–44) it is known that quasiparticles can “feel” a spatial variation of the superconducting order parameter as a kind of potential barrier. This physical mechanism (referred to as Andreev mechanism below) is the basis for Andreev quantization investigated previously for the core of a single vortex for the mixed state of a type-II superconductor<sup>43</sup> and for an isolated normal region of the intermediate state of a type-I superconductor<sup>44</sup> (or for a similar case of SNS contacts<sup>42</sup>). Based on our consideration of Sec. III B, one can expect that Andreev-type states can play a remark-

able role in superconducting nanograins due to significant spatial variations of the superconducting order parameter. This is very similar to recently investigated Andreev-type states in superconducting nanowires/nanofilms<sup>14,45</sup>, where the pair condensate is position dependent in the direction perpendicular to the nanowire/nanofilm due to the quantization of the perpendicular electron motion. In Ref. 45 it was shown that

$$\Delta_i = \int d^3r \Delta(\mathbf{r}) \left[ |u_i(\mathbf{r})|^2 + |v_i(\mathbf{r})|^2 \right], \quad (18)$$

which means that the pairing energy gap  $\Delta_i$  is the averaged value of the order parameter “watched” by the quasiparticles with quantum numbers  $i$ . Note that  $|u_i(\mathbf{r})|^2 + |v_i(\mathbf{r})|^2$  can be interpreted as the spatial distribution of quasiparticles according to the well-known constraint  $\int d^3r (|u_i(\mathbf{r})|^2 + |v_i(\mathbf{r})|^2) = 1$  [see, e.g., Ref. 35 and Eq. (10)]. When inserting Eqs. (6) into Eq. (18), one can easily obtain Eq. (12) with  $\Delta_i = \Delta_{jl}$ . If quasiparticles avoid the domains of enhanced pair condensate, the corresponding integral in the right-hand-side of Eq. (18) becomes smaller and, hence, such quasiparticles have smaller pairing gaps  $\Delta_{jl}$ . They can be referred to as Andreev-type states.

Our numerical study of quantum-number dependent pairing gaps  $\Delta_{jl}$  for metallic nanograins reveals a significant role of Andreev mechanism. Let us consider  $D = 13.52$  nm, the corresponding spatial distribution of the pair condensate is given in Fig. 3(b). To show how different species of quasiparticles are distributed in the radial direction in this case, the radial-dependent shell contributions (at  $T = 0$ )  $\Delta^{(jl)}(\rho)$  [see Eqs. (16) and (17)] are plotted in Fig. 5(a). We remark that such a representation is more informative than simply a plot of  $|u_{jl}(\rho)|^2 + |v_{jl}(\rho)|^2$ . First, the radial dependence of  $\Delta^{(jl)} \propto \chi_{jl}^2(\rho)$  is the same as that of  $|u_{jl}(\rho)|^2 + |v_{jl}(\rho)|^2 \propto \chi_{jl}^2(\rho)$  [see Eq. (8)]. Second, a plot of  $\Delta^{(jl)}(\rho)$  gives also information how the corresponding states contribute to  $\Delta(\rho)$ . From Fig. 3(c) we can see that a significant enhancement of the order parameter occurs at  $\rho/R = 0.45$ – $0.7$ . From Fig. 5(a) it is clear that this enhancement



is due to the states with  $(j, l) = (14, 48)$  and  $(9, 63)$ . Other shells, i.e.,  $(27, 16)$  and  $(23, 25)$  contribute less, and the corresponding quasiparticles, representing Andreev-type states, are mainly located beyond the domain  $\rho = 0.45 - 1.0$ . As a result, they have smaller pairing gaps, i.e.,  $\Delta_{27,16} = 2.65 \Delta_B$  and  $\Delta_{23,25} = 2.81 \Delta_B$ , as compared to  $\Delta_{14,48} = 4.098 \Delta_B$  and  $\Delta_{9,63} = 5.77 \Delta_B$ . As seen, the quasiparticles with  $(j, l) = (27, 16)$  are most successful in avoiding the local enhancement of  $\Delta(\rho)$  at  $\rho/R = 0.45-0.7$  and, so,  $\Delta_{27,16}$  is the smallest pairing gap. Such a manifestation of Andreev mechanism is not a particular feature of  $D = 13.52$  nm. In general,  $\Delta_{jl}$  strongly varies with  $j$  and  $l$  for diameters  $< 30 - 40$  nm, i.e., where spatial variations of the order parameter are still pronounced. Quite often such variations can be an order of magnitude, as, e.g., for  $D = 14.2$  nm (see  $\Delta(\rho)$  given in Fig. 2(c)). At this diameter a great enhancement of  $\Delta(\rho)$  takes place at  $\rho/R = 0.9$ . This is due to the contribution of the shell with  $(j, l) = (1, 101)$  [see Fig. 5(b)]. Other shells make much less important inputs and the corresponding quasiparticles are mainly distributed beyond the domain  $\rho/R = 0.9-1.0$ . So, as compared to  $\Delta_{1,101} = 9.32 \Delta_B$ , they have significantly smaller pairing gaps, i.e.,  $\Delta_{31,11} = 1.6 \Delta_B$ ,  $\Delta_{23,29} = 1.62 \Delta_B$ ,  $\Delta_{19,39} = 1.72 \Delta_B$  and  $\Delta_{8,71} = 2.35 \Delta_B$ . Thus, the interplay of Andreev mechanism and quantum confinement is responsible for variations of  $\Delta_{jl}$  with the relevant quantum numbers.

One could expect that such a serious difference in pairing gaps of different quasiparticle species can result in a pronounced drop of the ratio of  $\Delta_E$  (the minimal energy gap) to the critical temperature  $k_B T_c$ , similar to the case for quantum superconducting nanowires.<sup>14</sup> The main idea here is that  $\Delta_E$  is governed by Andreev-type states and, hence, is decreased. Unlike  $\Delta_E$ ,  $T_c$  is controlled by the quasiparticles making a major contribution to  $\Delta(\rho)$  and, so,  $T_c$  is coupled to their higher pairing gaps. As a result,  $\Delta_E/k_B T_c$  can be significantly smaller than in bulk. For instance, one can expect that  $\Delta_E = \Delta_{31,11} = 1.6 \Delta_B$  at  $D = 14.2$  nm while  $T_c$  is governed by  $\Delta_{1,101} = 9.32 \Delta_B$ . However, this is not correct for nanograins. The point is that  $\Delta_E$  is a spectroscopical gap which is probed by STM. It is defined as  $\Delta_E = \min_{jl} E_{jl}$ . For nanowires the subband-dependent pairing gap is always the minimal quasiparticle energy due to a quasi-free spectrum in the direction parallel to the nanowire. For nanograins this is different. In particular, for  $D = 14.2$  nm we have the following single-electron energies (absorbing  $\mu$ ) of the relevant shells:  $\xi_{31,11} = -18.6 \Delta_B$ ,  $\xi_{23,29} = -26.03 \Delta_B$ ,  $\xi_{19,39} = 20.9 \Delta_B$ ,  $\xi_{8,71} = 22.6 \Delta_B$  and  $\xi_{1,101} = 0$ . Hence, one can calculate that  $\Delta_E = E_{1,101} = \Delta_{1,101}$  in spite of the fact that  $\Delta_{1,101}$  is the largest pairing gap. Thus, although Andreev mechanism plays a significant role in superconducting nanograins, it can hardly be probed by STM-measurements due to the nonzero interlevel spacing, unlike quantum superconducting nanowires.

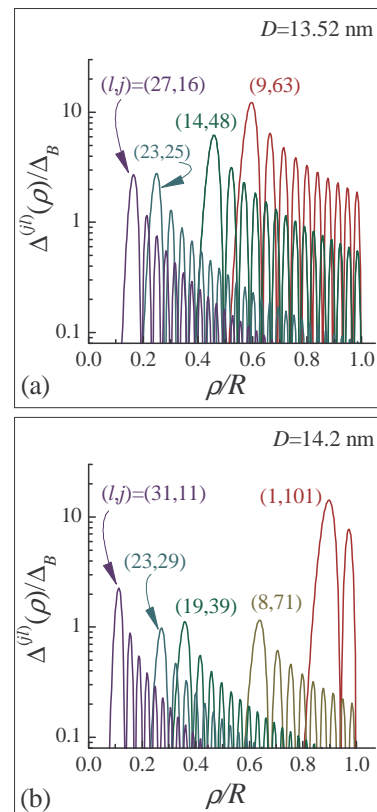


FIG. 5. Shell-dependent contributions to the order parameter  $\Delta_{jl}(\rho)$  for relevant shells: (a),  $D = 13.52$  nm,  $(j, l) = (27, 16)$ ,  $(23, 25)$ ,  $(14, 48)$  and  $(9, 63)$ ; (b)  $D = 14.2$  nm,  $(j, l) = (31, 11)$ ,  $(23, 29)$ ,  $(19, 39)$ ,  $(8, 71)$  and  $(1, 101)$ .

#### IV. CONCLUSIONS AND DISCUSSION

In conclusion, we have shown that the spatial distribution of the pair condensate is essentially nonuniform in metallic nanograins. In particular, the spatially nonuniform pairing can proliferate in nanograins even when  $k_F D \sim 300$  and, so, the usual criterion to neglect variations of the superconducting condensate with position, i.e.,  $k_F D \gg 1$ , is not very useful and can result in wrong conclusions. This is the reason why effects due to spatially nonuniform pairing in superconducting grains were previously overlooked. Our study suggests that a new criterion should be based on a more delicate energy scale (as compared to the Fermi energy), which, in the superconducting state, is given by the bulk order parameter  $\Delta_B$ . It turns out that the pairing becomes spatially nonuniform when the interlevel spacing  $\delta$  exceeds  $0.1-0.2 \Delta_B$ . Variations of the order parameter with position exhibit a pronounced enhancement with an increase of  $\delta/\Delta_B$ . When  $\delta \sim \Delta_B$ , such variations can be almost an order of magnitude in highly symmetric grains. At first sight, this seems impossible because it costs extra energy for such spatial variations. However, a nonuniform distribution of the pair condensate is accompanied

by enhanced pairing interaction matrix elements, which compensates the energy cost for an inhomogeneous distribution of the condensate. Another point is the size-dependent pinning of the chemical potential to groups of degenerate or nearly degenerate energy levels. Such a pinning plays the role of a filter that increases the contribution of the single-electron levels in the vicinity of the chemical potential and suppresses contributions of other states. This results in an additional mechanism favoring spatially nonuniform pairing in metallic nanograins.

In this paper we investigated a highly symmetric confining geometry. Due to this feature the problem becomes effectively one-dimensional (the order parameter depends only on the radial coordinate) and, so, sufficiently large diameters up to  $D \approx 40$  nm can be investigated. This size is almost impossible to reach theoretically for grains with the order parameter depending on three relevant coordinates due to time consuming numerical calculations. Such an effectively one-dimensional problem has large degeneration factors for the corresponding shell structure, resulting in a significant enhancement of the pairing correlations. In reality there can be several issues that may lead to a splitting of the shell levels. It will decrease the degeneration factors and, so, reduce the pairing correlations, since the main contribution to the sum in the gap equation comes from the transitions within the same shell pinned to the chemical potential. Among such issues is the Jahn-Teller deformation, i.e., the transformation of a spherical nanograin with incompletely filled shells to an ellipsoidal shape. In addition, the surface imperfections and impurities can significantly change the distribution of single-electron levels. However, our qualitative results are quite generic and do not depend on a particular shape of a nanograin and the presence of possible imperfections. For instance, when  $\delta \sim \Delta_B$  the pair condensate will always be spatially nonuniform because only a few single-electron levels enters the energy interval  $\approx [\mu - \Delta_B, \mu + \Delta_B]$ . Due to the dominant contribution of such levels to  $\Delta(\mathbf{r})$ , one can expect that the pair condensate acquires a profile governed by the squared absolute value of the wave function for the single-electron state closest in energy to  $\mu$ . This is significantly strengthened by an increase (in absolute value) of the diagonal matrix elements  $\langle i, \bar{i} | \Phi | i, \bar{i} \rangle$  and, in addition, by the pinning of the chemical potential to the single-particle levels.

We remark that the diagonal matrix elements, i.e.,  $\langle i, \bar{i} | \Phi | i, \bar{i} \rangle$  [see the definition for  $\Phi$  below Eq. (3)] are always enhanced as compared to  $-g/V$  in the presence of quantum confinement, whatever disorder and shape imperfections. This can be seen from the following simple arguments. Introducing  $\varphi_i(\mathbf{r})$ , the wave function associated with state  $i$ , one can write

$$\langle i, \bar{i} | \Phi | i, \bar{i} \rangle = -g \int d^3r |\varphi_i(\mathbf{r})|^4.$$

Due to the normalization condition we have  $|\varphi_i(\mathbf{r})|^2 = \frac{1}{V} + d_i(\mathbf{r})$ , where  $\int d^3r d_i(\mathbf{r}) = 0$ . Then, the above matrix

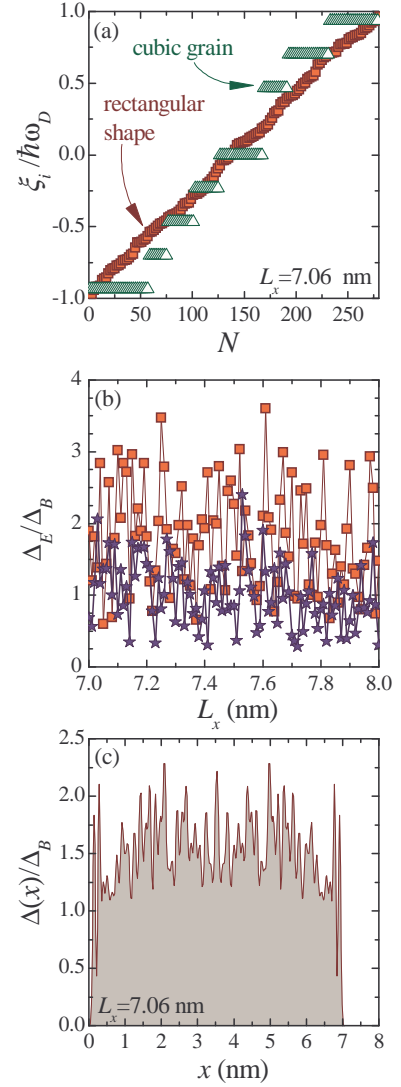


FIG. 6. (a) Single-electron energies  $\xi_i$  (given in units of the Debye energy  $\hbar\omega_D$ ) ordered in ascending manner versus the ordering number  $N$  for the rectangular-shaped aluminum nanograin with  $L_x = 7.06$  nm,  $L_y = L_x/1.1$ ,  $L_z = 1.1 L_x$  (squares) and for a cubic nanograin with  $L_x = 7.06$  nm (triangles). (b) The size-dependent excitation gap  $\Delta_E/\Delta_B$  versus  $L_x$  (in steps of  $\delta L_x = 0.01$  nm) for an aluminum nanograin of the rectangular shape with the dimensions  $L_x, L_y = L_x/1.1, L_z = 1.1 L_x$ : squares represent the results calculated with the modified matrix elements and with proper variations of  $\mu$ ; stars are the data obtained for the bulk-like matrix elements  $-g/V$  and  $\mu = \mu_B$ . (c) The spatial distribution of the pair condensate in the rectangular grain with  $L_x = 7.06$  nm and  $L_y = L_x/1.1, L_z = 1.1 L_x$ ,  $\Delta(x) = \Delta(x, y, z)|_{y=x/1.1, z=1.1x}$ .

element can be rearranged as

$$\langle i, \bar{i} | \Phi | i, \bar{i} \rangle = -\frac{g}{V} \left[ 1 + V \int d^3r d_i^2(\mathbf{r}) \right].$$

The second term in the brackets is always positive in the presence of quantum confinement, i.e., when  $d_i(\mathbf{r}) \neq 0$ .

It is zero only when  $\varphi_i(\mathbf{r})$ 's are chosen in the form of plane waves, which results in  $\langle \bar{i}, \bar{i} | \Phi | i, \bar{i} \rangle = -g/V$ .

The above discussion can be supplemented by our numerical results calculated from the BCS-like equation similar to Eq. (15) but now for aluminum nanograins of rectangular shape with dimensions  $L_x, L_y = L_x/1.1, L_z = 1.1L_x$ . For aluminum we have<sup>32,36,37</sup>:  $\hbar\omega_D/k_B = 375$  K,  $gN(0) = 0.18$ , and  $\mu_B = 11.67$  eV, which corresponds to the electron density  $n_e = 181$  nm<sup>-3</sup>. In Fig. 6(a) single-electron levels arranged in the ascending order are shown within the Debye window for the rectangular nanograin with  $L_x = 7.06$  nm (squares). The same is also given here for a cubic aluminum nanograin with  $L_x = L_y = L_z = 7.06$  nm (triangles). As seen, single-electron levels for the rectangular shape are distributed in a nearly equidistant manner (with  $\delta \approx 0.2$ - $0.3$  meV  $\sim \Delta_B$ ) contrary to the states corresponding to the cubic geometry. It is well-known that an almost equidistant distribution<sup>4</sup> of single-electron levels near  $\mu$  is also expected in the presence of significant imperfections such as the surface roughness and/or impurities. So, our results in Fig. 6 give a feeling about the role of the spatially nonuniform pairing in disordered metallic grains. The excitation energy gap  $\Delta_E$  for the rectangular nanograin is shown in units of  $\Delta_B$  in Fig. 6 as a function of  $L_x$  in the interval  $L_x = 7$ - $8$  nm. Here squares represent our results calculated with the modification of the matrix elements and with  $\mu$  varying with

$L_x$ ; stars are the results found for the bulk-like matrix elements  $-g/V$  and  $\mu = \mu_B$ . As seen,  $\Delta_E$  ( $\propto T_c$ ) is now two-times enhanced as compared to  $\Delta_B$  (on average), which is much less significant than for highly symmetric grains (compare with Fig. 1) due to a splitting of the shell levels. However, the effect of interest is still pronounced:  $\Delta_E$  calculated for the modified matrix elements and with account of size variations of  $\mu$  is generally larger by a factor of 1.5-2.0. The spatial profile of the order parameter is nonuniform with local enhancements over its average value by about 100%, see, e.g., Fig. 6(c). For rectangular grains with  $L_x = 7$ - $8$  nm we have  $\delta \sim \Delta_B$ . However, as we checked, the spatially nonuniform pairing and the related effects of the modification of the relevant matrix elements and the size-dependent pinning of  $\mu$  are of significance even for smaller  $\delta$ 's, i.e., when  $\delta > 0.1$ - $0.2\Delta_B$  ( $L_x < 14$ - $15$  nm). For instance, at  $L_x = 11$  nm the order parameter exhibits variations of about 30-40% of its averaged value. These results are in agreement with our expectations based on the investigation of the highly symmetric spherical grains.

## ACKNOWLEDGMENTS

This work was supported by the Alexander von Humboldt Foundation, the Flemish Science Foundation (FWO-VI) and the Belgian Science Policy (IAP).

- 
- <sup>1</sup> R. Parmenter, Phys. Rev. **166**, 392 (1968).  
<sup>2</sup> J. M. Blatt and C. J. Thompson, Phys. Rev. Lett. **10**, 332 (1963).  
<sup>3</sup> B. Mühlischlegel, D. J. Scalapino, and R. Denton, Phys. Rev. B **6**, 1767 (1972).  
<sup>4</sup> R. A. Smith, and V. Ambegaokar, Phys. Rev. Lett. **77**, 4962 (1996).  
<sup>5</sup> A. Perali, A. Bianconi, A. Lanzara and M. L. Saini, Solid State Commun. **100**, 181 (1996).  
<sup>6</sup> F. Braun and J. von Delft, Phys. Rev. B **59**, 9527 (1999).  
<sup>7</sup> G. Sierra, J. Dukelsky, G. G. Dussel, J. von Delft, and F. Braun, Phys. Rev. B **61**, R11890 (2000).  
<sup>8</sup> V. N. Gladilin, V. M. Fomin, and J. T. Devreese, Solid State Commun. **121**, 519 (2002).  
<sup>9</sup> E. A. Yuzbashyan, A. A. Baytin, and B. L. Altshuler, Phys. Rev. B **68**, 214509 (2003).  
<sup>10</sup> Y. N. Ovchinnikov and V. Z. Kresin, Eur. Phys. J. B **45**, 5 (2005); *ibid*, Eur. Phys. J. B **47**, 333 (2005).  
<sup>11</sup> V. Z. Kresin and Y. N. Ovchinnikov, Phys. Rev. B **74**, 024514 (2006).  
<sup>12</sup> A. A. Shanenko and M. D. Croitoru, Phys. Rev. B **73**, 012510 (2006).  
<sup>13</sup> M. D. Croitoru, A. A. Shanenko, and F. M. Peeters, Phys. Rev. B **76**, 024511 (2007).  
<sup>14</sup> A. A. Shanenko, M. D. Croitoru, R. G. Mints, and F. M. Peeters, Phys. Rev. Lett. **99**, 067007 (2007).  
<sup>15</sup> A. A. Shanenko, M. D. Croitoru, and F. M. Peeters, Phys. Rev. B **78**, 024505 (2008).  
<sup>16</sup> M. D. Croitoru, A. A. Shanenko, C. C. Kaun, and F. M. Peeters, Phys. Rev. B **80**, 024513 (2009).  
<sup>17</sup> A. M. García-García, J. D. Urbina, E. A. Yuzbashyan, K. Richter, and B. L. Altshuler, Phys. Rev. Lett. **100**, 187001 (2008).  
<sup>18</sup> I. Giaever and H. R. Zeller, Phys. Rev. Lett. **20**, 1504 (1968); H. R. Zeller and I. Giaever, Phys. Rev. **181**, 789 (1969).  
<sup>19</sup> W.-H. Li, C. C. Yang, F. C. Tsao, S. Y. Wu, P. J. Huang, M. K. Chung, and Y. D. Yao, Phys. Rev. B **72**, 214516 (2005).  
<sup>20</sup> W.-H. Li, C.-W. Wang, C.-Y. Li, C. K. Hsu, C. C. Yang, and C.-M. Wu, Phys. Rev. B **77**, 094508 (2008);  
<sup>21</sup> S. Bose, P. Raychaudhuri, R. Banerjee, P. Vasa, and P. Ayyub, Phys. Rev. Lett. **95**, 147003 (2005).  
<sup>22</sup> S. Bose, C. Galande, S. Chockalingam, R. Banerjee, P. Raychaudhuri, and P. Ayyub, J. Phys.: Condens. Matter **21**, 205702 (2009).  
<sup>23</sup> D. C. Ralph, C. T. Black, and M. Tinkham, Phys. Rev. Lett. **74**, 3241 (1995).  
<sup>24</sup> C. T. Black, D. C. Ralph, and M. Tinkham, Phys. Rev. Lett. **76**, 688 (1996).  
<sup>25</sup> I. Brihuega, S. Bose, M. M. Ugeda, C.H. Michaelis, and K. Kern, arXiv: 0904.0354, April 2009.  
<sup>26</sup> S. Bose, A. M. García-García, M. M. Ugeda, J. D. Urbina, C. H. Michaelis, and K. Kern, Nature Mat. **9**, 550 (2010).  
<sup>27</sup> J. von Delft, A. D. Zaikin, D. S. Golubev, and W. Tichy, Phys. Rev. Lett. **77**, 3189 (1996).  
<sup>28</sup> K. A. Matveev and A. I. Larkin, Phys. Rev. Lett. **78**, 3749 (1997).

- <sup>29</sup> Small corrections to  $-\frac{g}{V}$  of about 1%–3% were considered in Ref. 17 for chaotic grains.
- <sup>30</sup> Impact of a shell structure on superconducting correlations were previously considered within the grand canonical formalism in Refs. 10 and 11 and 17 and 25. However, the authors of Refs.<sup>10,11</sup> did not investigate the dependence of the relevant matrix elements on quantum numbers (and, so, ignored the spatial dependence of the pair condensate entirely) but took account of the pinning of the chemical potential to incomplete shells. In Refs. 17 and 25 neither modifications of the matrix elements due to quantum confinement nor the quantum-size pinning of the chemical potential were considered.
- <sup>31</sup> N. N. Bogoliubov, *Sov. Phys.-Usp.* **2**, 236 (1959) [see, also, N. N. Bogoliubov, *Selected Works, Part II, Quantum and Classical Statistical Mechanics*(Gordon and Breach, Amsterdam, 1991)].
- <sup>32</sup> P. G. de Gennes, *Superconductivity of Metals and Alloys* (W. A. Benjamin, New York, 1966).
- <sup>33</sup> A. V. Swidzinsky, *Spatially Inhomogeneous Problems in the Theory of Superconductivity* (Nauka, Moscow, 1982).
- <sup>34</sup> P. W. Anderson, *J. Phys. Chem. Solids* **11**, 26 (1959).
- <sup>35</sup> J. B. Ketterson and S. N. Song, *Superconductivity* (Cambridge Univ. Press., Cambridge, 1999).
- <sup>36</sup> A. L. Fetter and J. D. Walecka, *Quantum Theory of Many-Particle Systems* (Dover, New York, 2003).
- <sup>37</sup> N. W. Ashcroft and N. D. Mermin, *Solid State Physics* (Saunders, 1976).
- <sup>38</sup> Y. Guo, Y. F. Zhang, X. Y. Bao, T. Z. Tang, L. X. Zhang, W. G. Zhu, E. G. Wang, Q. Niu, Z. Q. Qiu, J. F. Jia, Z. X. Zhao, and Q. K. Xue, *Science* **306**, 1915 (2004).
- <sup>39</sup> D. Eom, S. Qin, M. Y. Chou, and C. K. Shih, *Phys. Rev. Lett.* **96**, 027005 (2006); S. Y. Qin, J. Kim, Q. Niu, and C. K. Shih, *Science* **324**, 1314 (2009).
- <sup>40</sup> W. Satula, J. Dobaczewski, and W. Nazarewicz, *Phys. Rev. Lett.* **81**, 3599 (1998).
- <sup>41</sup> J.-P. Martikainen and P. Törma, *Phys. Rev. Lett.* **95**, 170407 (2005).
- <sup>42</sup> P. G. de Gennes, and D. Saint-James, *Phys. Lett.* **4**, 151 (1963).
- <sup>43</sup> C. Caroli, P. G. de Gennes, and J. Matricon, *Phys. Lett.* **9**, 307 (1964).
- <sup>44</sup> A. F. Andreev, *Sov. Phys. JETP* **22**, 455 (1966).
- <sup>45</sup> A. A. Shanenko, M. D. Croitoru, and F. M. Peeters, *Phys. Rev. B* **78**, 054505 (2008).